Photophysics and Nonlinear Optical Properties of Tetra- and Octabrominated Silicon Naphthalocyanines

Yunjing Li,[†] Danilo Dini,[‡] Mario J. F. Calvete,[‡] Michael Hanack,[‡] and Wenfang Sun*[,†]

Department of Chemistry, Biochemistry and Molecular Biology, North Dakota State University, Fargo, North Dakota 58105-5516, and Institute of Organic Chemistry, University of Tübingen, Auf der Morgenstelle 18, D-72076 Tübingen, Germany

Received: September 4, 2007; In Final Form: October 24, 2007

The effect of the number of bromide substituents on the photophysical and nonlinear optical properties of the tetrabrominated naphthalocyanine $Br_4(tBu_2PhO)_4NcSi[OSi(Hex)_3]_2$ (**1**) and the octabrominated naphthalocyanine $Br_8NcSi[OSi(Hex)_3]_2$ (**2**) has been investigated through various spectroscopic techniques. Absorption and emission of **1** and **2** have been studied at room temperature and 77 K to determine the spectral properties of the ground and the excited states and the lifetimes and quantum yields of formation of the excited states. There is a moderate increase of the quantum yield of the triplet excited-state formation ($\Phi_T = 0.10$ vs 0.13) and a decrease of the triplet excited-state lifetime ($\tau_T \approx 70$ vs 50 μs) from **1** to **2**. These can be attributed to the stronger heavy atom effect produced by the larger number of peripheral bromide substituents in **2** considering that an excited state with a triplet manifold is involved in the excitation dynamics of both complexes **1** and **2**. The quantum yields of the singlet oxygen formation (Φ_Δ) upon irradiation of **1** and **2** at 355 nm were also evaluated, and a value of $\Phi_\Delta(\mathbf{1}) = \Phi_\Delta(\mathbf{2}) = 0.16$ was obtained. In addition to that, octabrominated complex **2** displays a larger decrease of nonlinear optical transmission for nanosecond pulses at 532 nm with respect to the tetrabrominated complex **1**. The nanosecond Z-scan experiments reveal that **1** and **2** exhibit both a reverse saturable absorption and a nonlinear refraction at 532 nm. However, both the sign and the magnitude of the nonlinear refraction change from **1** to **2**. For picosecond Z-scan in the visible spectral region, these two complexes exhibit only reverse saturable absorption, and the excited-state absorption cross-section increases at longer wavelengths.

Introduction

Naphthalocyanines (Nc's) are complexes that possess an extended network of 56 conjugated π-electrons and display a sharp absorption peak with large values of the molar extinction coefficient (on the order of 10^5 M^{-1} cm^{-1}) within the spectral range of 700−1000 nm.[1] Nc's have found numerous applications in materials science and advanced technologies, e.g., as nonlinear optical materials,[2] semiconducting materials,[3] photosensitizers for photodynamic therapy (PDT) of cancers,[4] electrocatalysts for water reduction,[5] photoconductors,[6] NIR-emitting materials,[7] and active materials in NIR-readable inks[8] and in thin film applications.[9] More recently, Nc's have also been employed in holographic storage[10] and high-resolution IR imaging.[11] Such a variety of applications is owed to the versatility, high yields, and ease of the synthesis of Nc's,[12] which lead to various structural variations that differ in the central atom, the axial ligands, and the nature and numbers of peripheral substituents. As a consequence, the chemical-physical properties of the resulting Nc's can be largely modulated depending on the choice of the predefined structural factors.

In this work we have synthesized two new silicon naphthalocyanines (Chart 1), namely, [3(4),12(13),21(22),30(31)-tetrabromo-4(3),13(12),22(21),31(30)-tetrakis(3,5-di-*tert*-butylphenoxy)naphthalocyaninato]bis(trihexylsiloxy)silane {$Br_4(tBu_2PhO)_4NcSi[OSi(Hex)_3]_2$} (**1**) and (3,4,12,13,21,22,30,31-octabromonaphthalocyaninato)bis(trihexylsiloxy)silane {$Br_8NcSi[OSi(Hex)_3]_2$} (**2**), which contain different numbers of bromide as the peripheral substituent.[13] The aim of this work is to evaluate how the number of heavy bromide substituents affects the excited-state characteristics of these two complexes and how these parameters influence their nonlinear optical properties and their efficiency to generate singlet oxygen.

The design of brominated naphthalocyanines **1** and **2** has been inspired by the favorable role that bromine plays in the kinetics of photoexcitation during the process of nonlinear absorption as recently verified with a peripherally brominated indium chloride naphthalocyanine.[13a,e] This study demonstrated that peripheral bromination in chloroindium(III) 3(4),12(13),21(22),-30(31)-tetrabromo-4(3),13(12),22(21),31(30)-tetrakis(3,5-di-*tert*-butylphenoxy)naphthalocyanine enhanced the photostability, accelerated the intersystem crossing rate, and increased the yield of excited-state formation upon irradiation with nanosecond laser pulses.[13a] An additional effect of peripheral bromination on the photophysical properties of this complex was the shortening of the triplet excited-state lifetime.[13a]

In contrast to the previously reported poorly soluble octabrominated naphthalocyanines with zinc and lead as the central metal (on the order of 10^{-5}−10^{-4} mol/L),[13c,d] the synthesized octabrominated complex **2** has achieved a much better solubility, being on the order of 10^{-2} mol/L in common organic solvents despite the presence of eight polar atoms in the structure of **2** (Chart 1). This feature would prevent the formation of long-

* To whom correspondence should be addressed. E-mail: wenfang.sun@ndsu.edu.
[†] North Dakota State University.
[‡] University of Tübingen.

10.1021/jp0771116 CCC: $40.75
Published on Web 12/29/2007

CHART 1: [3(4),12(13),21(22),30(31)-Tetrabromo-4(3),13(12),22(21),31(30)-tetrakis(3,5-di-*tert*-butylphenoxy)-naphthalocyaninato]bis(trihexylsiloxy)silane {$Br_4(tBu_2PhO)_4NcSi[OSi(Hex)_3]_2$, 1} and (3,4,12,13,21,22,30,31-Octabromonaphthalocyaninato]bis(trihexylsiloxy)silane {$Br_8NcSi[OSi(Hex)_3]_2$, 2}

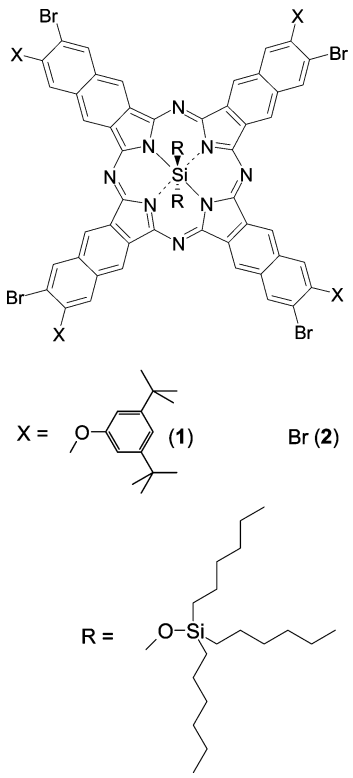

lived excited species due to molecular aggregation,[14] which could consequently reduce the excited-state absorption.[15] However, the molecular aggregation could be reduced by the presence of two bulky axial ligands such as $-OSi(C_6H_{13})_3$. As a result, a stabilization of the excited state is expected for naphthalocyanine **2** with respect to the other reported octabrominated naphthalocyanines with no axial substituents. In this framework silicon complex **2** can be considered as the first example of soluble octabrominated naphthalocyanine. In the structure of tetrabrominated silicon naphthalocyanine **1** (Chart 1), four bromide groups have been replaced by four di-*tert*-butylphenoxy groups to further increase the solubility. The presence of these bulky di-*tert*-butylphenoxy groups is also expected to further reduce the degree of aggregation even at a high concentration range ($>10^{-3}$ mol/L).[13a]

Experimental Section

Materials. Reference compounds silicon 2,3-naphthalocyanine bis(trihexylsilyl oxide) (SiNc) and zinc tetraphenylporphyrin (ZnTPP) were purchased from Aldrich and Alfa Aesar, respectively, and were used without further purification.

Synthesis. Naphthalocyanines **1** and **2** were synthesized through the direct reaction of the corresponding dihydroxy silicon complexes dihydroxysilicon(II) 3(4),12(13),21(22),30(31)-tetrabromo-4(3),13(12),22(21),31(30)-tetrakis(3,5-di-*tert*-butylphenyloxy)naphthalocyanine [$Br_4(tBu_2PhO)_4NcSi(OH)_2$, **3**] for **1** and dihydroxysilicon(II) 3,4,12,13,21,22,30,31-octabromonaphthalocyanine [$Br_8NcSi(OH)_2$, **4**] for **2**, with an excess of tri-*n*-hexylchlorosilane in DMF.

Synthesis of 3. 6-Bromo-7-[(3,5-di-*tert*-butyl)phenoxy]-1,3-diiminobenzo[*f*]isoindoline (**5**) was prepared from 6-bromo-7-[(3,5-di-*tert*-butyl)phenoxy]-2,3-dicyanonaphthalene by reaction with NH_3 in $NaOCH_3/CH_3OH$ according to a previously reported procedure.[13a] **5** (1.5 g, 3 mmol) and silicon tetrachloride (510.0 mg, 3 mmol) were mixed in dry chinoline (5 mL) and heated at 195 °C for 6 h (Scheme 1). After cooling, the reaction mixture was poured into methanol (200 mL) and stirred. Successive water (20 mL) was added, and the precipitates were collected and washed with methanol. The crude dark yellow-green solid was dissolved in 30 mL of a pyridine/water mixture (5:1, v/v) and heated at 100 °C for 30 min. The mixture was then poured into methanol (200 mL) and stirred. The precipitates were collected to give 0.40 g of **3** as a dark yellow green solid (yield 55%). MS-FAB (*m/z*): 1907.7 (M^+), 1817.5 ($M^+ - Br$). ^1H NMR (THF-d_8): δ 1.33 (s, br, 72H, CH_3), 7.06, 7.39 (br, 12H, phenoxy), 8.17, 8.28 (br, 8H on C-2), 10.81 (br, 8H on C-4) ppm. ^{13}C NMR (THF-d_8): δ 30.7 (CH_3), 34.9 (CCH_3), 114.6 (br, C-8, C-10), 118.9 (br, C-2,C-4), 134.2 (br, C-3, C-5), 135.3 (br, C-6), 153.3 (br, C-7), 155.5 (br, C-1) ppm.

SCHEME 1

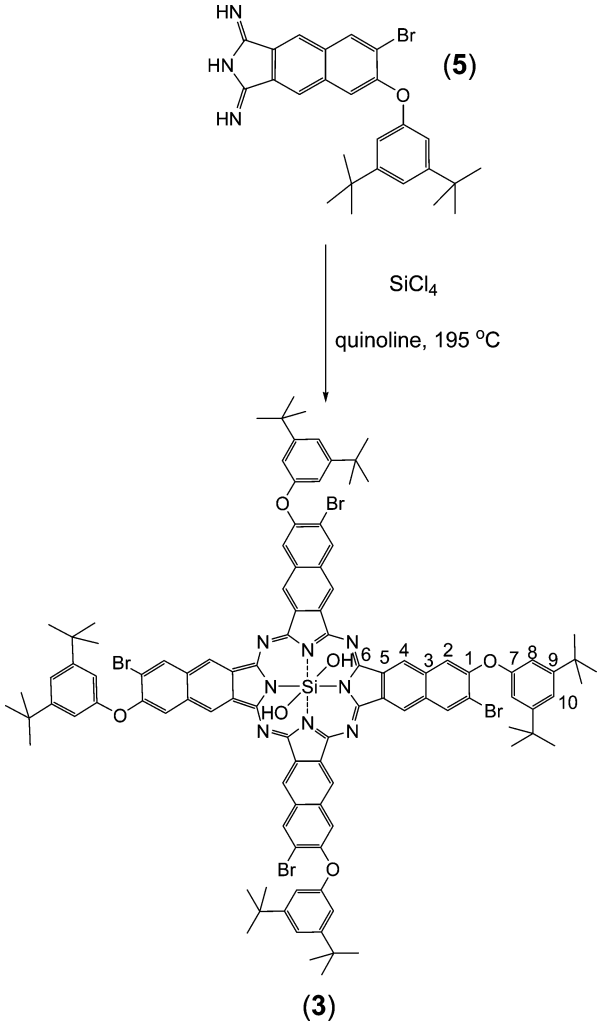

Synthesis of 1. A mixture of **3** (190 mg, 0.1 mmol), tri-*n*-hexylchlorosilane (96 mg, 0.3 mmol), imidazole (20 mg), and DMF (3 mL) was stirred at room temperature for 24 h. The resultant mixture was concentrated under vacuum with a rotary evaporator. The residue was chromatographed on silica gel using a mixture of dichloromethane/tetrahydrofuran (98:2, v/v) as the eluent. The first green fraction was collected, vacuum-dried, and weighed. A 180 mg portion of **1** was obtained (yield 72%). Tetrabrominated naphthalocyanine **1** thus prepared is actually a mixture of regioisomers that differ in the relative position of

SCHEME 2

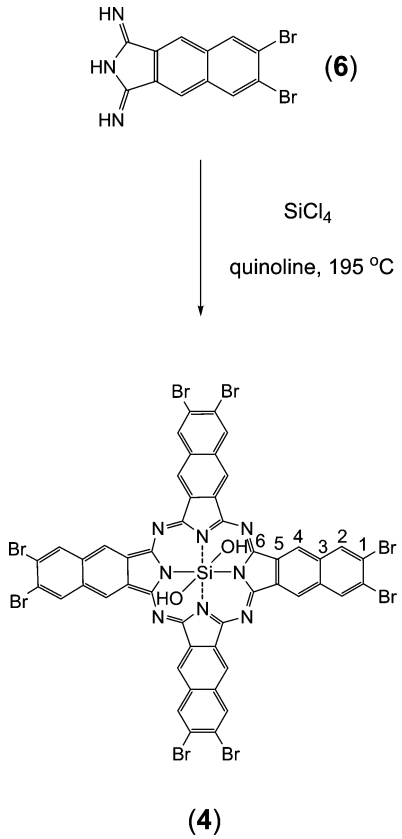

the two substituents (bromide and 3,5-di-*tert*-butylphenoxy). However, further chromatographic separation of these isomers was not conducted since the photophysical properties investigated should not be affected by the relative position of the substituents at the naphthalocyanine ring. MS-FAB (*m/z*): 2472.9 (M^+). ^{1}H NMR (THF-d_8): δ 0.56 (br, 12H, CH_2Si), 0.90 (br, 18H, CH_3), 1.30 (br, 48H, CH_2), 1.38 (s, br, 72H, phenoxy CH_3), 7.08, 7.38 (br, 12H, phenoxy), 8.18, 8.26 (br, 8H on C-2), 10.83 (br, 8H on C-4) ppm. ^{13}C NMR (THF-d_8): δ 14.0−32.1 (hexyl C), 30.7 (CH_3), 34.9 (C−CH_3), 114.6 (br, C-8, C-10), 118.9 (br, C-2, C-4), 134.2 (br, C-3, C-5), 135.3 (br, C-6), 153.3 (br, C-7), 155.5 (br, C-1) ppm.

Synthesis of ***4***. Silicon tetrachloride (114 μL, 1 mmol) was added to a solution of 6,7-dibromo-1,3-diiminobenzo[*f*]isoindoline (**6**) (433 mg, 1.3 mol)[13a] in freshly distilled chinoline (2 mL) under an argon atmosphere (Scheme 2). The mixture was heated to 210 °C and stirred for 2 h. The resultant product was slowly cooled and refluxed in 2 mL of water for 20 min. The mixture was cooled, washed with ether (4 mL), and filtered. The solid was then washed with 2 mL of ether twice. The dark green solid **4** was vacuum-dried and weighed (0.57 g, yield 73%). MS-FAB (*m/z*): 1406.2 (M^+), 1327.1 (M^+ − Br). ^{1}H NMR (THF-d_8): δ 7.06, 8.17, 8.28 (br, 8H on C-2), 10.81 (br, 8H on C-4) ppm. ^{13}C NMR (THF-d_8): δ 118.9 (br, C-2, C-4), 134.2 (br, C-3, C-5), 135.3 (br, C-6), 155.5 (br, C-1) ppm.

Synthesis of ***2***. A mixture of **4** (280 mg, 0.2 mmol), tri-*n*-hexylchlorosilane (160 mg, 0.5 mmol), imidazole (40 mg), and dimethylformamide (5 mL) was stirred at room temperature for 24 h. The resultant mixture was concentrated under vacuum with a rotary evaporator. The residue was chromatographed on silica gel with a mixture of dichloromethane/tetrahydrofuran (95:5, v/v) as the eluent. The first green fraction was collected, vacuum-dried, and weighed to give 280 mg of **2** (yield 71%). MS-FAB (*m/z*): 1972.9 (M^+). ^{1}H NMR (THF-d_8): δ 0.56 (br, 12H, CH_2Si), 0.90 (br, 18H, CH_3), 1.30 (br, 48H, CH_2), 8.18, 8.26 (br, 8H on C-2), 10.83 (br, 8H on C-4) ppm. ^{13}C NMR (THF-d_8): δ 14.0−32.1 (hexyl C), 118.9 (br, C-2, C-4), 134.2 (br, C-3, C-5), 135.3 (br, C-6), 155.5 (br, C-1) ppm.

Photophysical Measurements. UV−vis spectra were measured with an Agilent 8453 UV−vis spectrophotometer using a 10 mm thick quartz cuvette. Benzene was used as the solvent. Steady-state fluorescence spectra at room temperature and 77 K were measured on a SPEX Fluorolog-3 fluorimeter and phosphorimeter. The excitation wavelength was selected in correspondence to the Q-band of each naphthalocyanine. Benzene was used as the solvent and was purged with argon for 30 min before each measurement.

The emission spectra at 77 K, the time-resolved triplet transient difference absorption spectra, and the lifetime of the triplet excited state were measured using an Edinburgh LP920 laser flash photolysis spectrometer. The third harmonic output (λ = 355 nm) of a Quantel Brilliant Nd:YAG laser was used as the excitation beam. The laser pulse width was 4.1 ns, and the frequency of the laser was adjusted to 3.3 Hz. The average energy of a single pulse was ~3 mJ. The concentrations of complexes **1** and **2** in benzene were typically on the order of several micromoles per liter, which provided an absorptivity of 0.4 in a 10 mm thick quartz cuvette at 355 nm. All samples were purged with argon before each experiment.

The molar extinction coefficients of the triplet excited state (ϵ_T) for Nc's **1** and **2** in benzene were measured by the singlet depletion method and calculated using the following equation:[16]

$$\epsilon_T = \frac{\epsilon_S[\Delta OD_T]}{\Delta OD_S} \quad (1)$$

where ΔOD_S and ΔOD_T are the absorbance of the triplet transient difference absorption spectrum at the minimum of the bleaching band and the maximum of the positive band, respectively, and ϵ_S is the ground-state molar extinction coefficient at the absorption band maximum.

The quantum yields of the triplet excited-state formation (Φ_T) for Nc's **1** and **2** were determined using the comparative method.[17] SiNc in benzene ($\Phi_T = 0.20 \pm 0.03$, $\epsilon_{T,590} = 53\,400$ M^{-1} cm^{-1}) was used as the reference.[4h] All the samples were optically matched at the excitation wavelength, and the triplet excited-state quantum yields were calculated using the following equation:

$$\Phi_T^s = \Phi_T^{ref}\frac{\Delta OD_T^s}{\Delta OD_T^{ref}}\frac{\epsilon_T^{ref}}{\epsilon_T^s} \quad (2)$$

where ΔOD_T^s and ΔOD_T^{ref} are the maximum optical density changes during transient absorption due to the triplet−triplet transition of the studied sample and the reference, respectively, ϵ_T^{ref} and ϵ_T^s are the molar extinction coefficients of this transition at the wavelength where OD_T is observed for the reference and the sample, respectively, and Φ_T^{ref} is the triplet excited-state quantum yield of the reference.

Singlet Oxygen Quantum Yield Measurement. The emission of singlet oxygen produced during the sample excitation process was measured using a LP900 singlet oxygen spectrometer. All measurements were carried out at room temperature in air-saturated benzene solutions. A liquid-nitrogen-cooled germanium (Ge) detector was used to monitor the emission signal in the NIR spectral range. Sample excitation was provided by the third-harmonic output (355 nm) of the Nd:YAG laser

described in the previous section with the repetition rate set at 1 Hz. The average energy of a single laser pulse was 2 mJ. The concentrations of all samples were adjusted to obtain the same absorbance (*A*) value of 0.5 at 355 nm. The singlet oxygen quantum yield was then determined by the comparative method.[4h] The integrated singlet oxygen emission intensity of **1** and **2** was compared to that of the optically matched reference sample (SiNc, $\Phi_\Delta = 0.19 \pm 0.02$),[4h] and the singlet oxygen quantum yield was then calculated according to the following equation:

$$\Phi_\Delta^s = \Phi_\Delta^{ref} \frac{G_\Delta^s}{G_\Delta^{ref}} \frac{A_{ref}}{A_s} \quad (3)$$

where G_Δ is the integrated singlet oxygen emission intensity and *A* is the absorbance at 355 nm. The suffixes "s" and "ref" refer to the sample and the reference, respectively.

Nonlinear Transmission Measurements. The experimental setup for nonlinear transmission measurements has been described previously.[18] The second harmonic of a 4.1 ns, Q-switched Quantel Brilliant Nd:YAG laser ($\lambda = 532$ nm) was used as the light source. The frequency was set at 10 Hz. The laser beam was focused by an $f = 30$ cm planoconvex lens to the center of a 2 mm thick quartz cuvette that contained the sample solution. The radius of the beam waist was approximately 75 μm. Two Molectron J4-09 pyroelectric probes and an EPM2000 energy/power meter were used to monitor the incident and output energies.

Z-Scan Measurements. The Z-scan experimental setup has been described previously.[19] The Quantel Brilliant Nd:YAG laser with a pulse width of 4.1 ns and a repetition rate of 10 Hz and an EKSPLA PG401 optical parametric generator (OPG) pumped by a PL2143A passively model-locked, Q-switched Nd:YAG laser with a pulse width of 27 ps and a repetition rate of 10 Hz were used as the light source for the nanosecond and picosecond experiments, respectively. The laser beam was focused by a 30 cm focal length planoconvex lens for the nanosecond measurement and by a 25 cm focal length planoconvex lens for the picosecond measurement, which gave rise to beam waists of 33 and 42 μm at the focal point, respectively. These beam waists result in Rayleigh lengths ($z_0 = \pi\omega_0^2/\lambda$, where ω_0 is the radius at the beam waist) of 6.4 and 10.4 mm, respectively. Therefore, a 1 mm cuvette was used for the nanosecond Z-scan measurements and a 2 mm cuvette for the picosecond measurements. The energies used for the nanosecond and picosecond Z-scan measurement were 6.0 and 1.8 μJ/pulse, respectively.

Results and Discussion

Electronic Absorption Spectra. 1 and **2** exhibit similar UV−vis absorption spectra (shown in Figure 1). The Q-band displays a vibronic progression with the most intense peak appearing at 782 nm for **1** and 781 nm for **2**. The maximum of the B-band is located at 358 and 361 nm for **1** and **2**, respectively. Both complexes obey Beer's law in dilute solutions, i.e., 7.4×10^{-6} to 2.4×10^{-4} mol/L for **1** and 4.0×10^{-6} to 4.5×10^{-5} mol/L for **2**. Octabrominated complex **2** displays a broadening of the Q(0,0) band and a decrease of the ϵ value when the concentration is increased from 4.5×10^{-5} to 2.3×10^{-4} mol/L (Figure 1b). This indicates the occurrence of molecular aggregation for naphthalocyanine **2** even at these concentration values.[13a,14] A similar phenomenon is observed for complex **1**, but at much higher concentrations, i.e., $C \geq 2.4 \times 10^{-4}$ mol/L.

Emission. Figure 2 displays the steady-state emission spectra of **1** and **2** at room temperature. Both spectra exhibit a vibronic

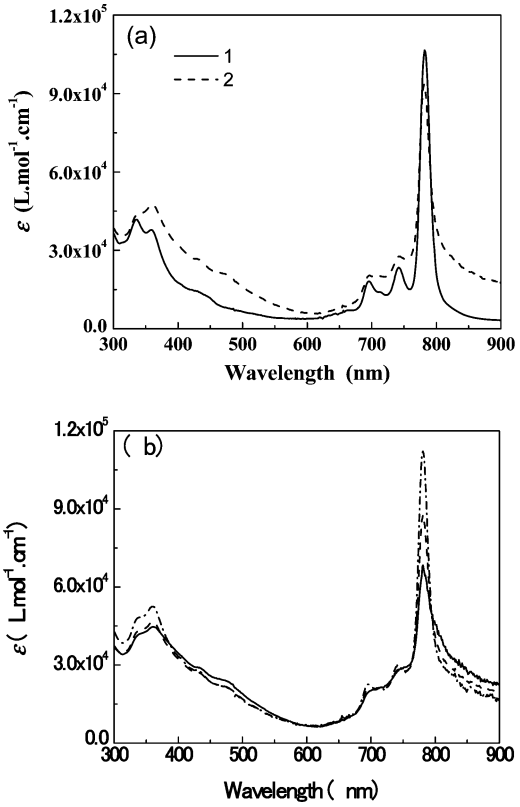

Figure 1. (a) UV−vis absorption spectra of **1** and **2** in benzene. (b) Spectral variation of ϵ with concentration (*C*) for **2** in benzene: $C = 2.3 \times 10^{-4}$ mol/L (solid line); $C = 1.6 \times 10^{-5}$ mol/L (dashed line); $C = 4.0 \times 10^{-6}$ mol/L (dashed−dotted line).

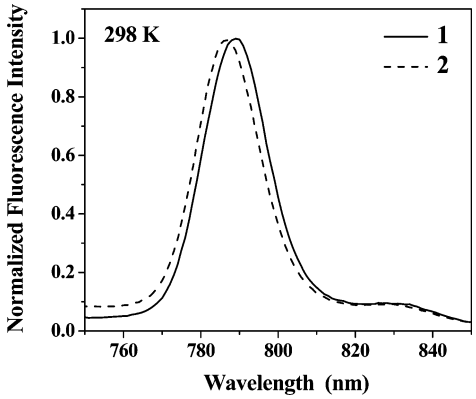

Figure 2. Normalized fluorescence spectra of **1** and **2** at room temperature in benzene. The excitation wavelength is 695 nm for **1** and 696 nm for **2**.

structure with a progression spacing of 611 cm^{-1} for **1** and 629 cm^{-1} for **2**. The shape of the emission spectra is almost a mirror image of the Q-band of the UV−vis absorption spectra, and the vibronic progression spacing of the emission spectra coincides with the spacing separation between the Q(0,0) band and the Q(0,1) band. These features imply that the emission observed at room temperature originates from the first singlet excited state; namely, it is fluorescence. This notion is supported by the emission lifetime measurement of these two complexes. As listed in Table 1, the emission for both complexes exhibits a biexponential decay, with a shorter lifetime of ~2 ns and a longer one of ~6 ns.

The time-resolved emission spectra at 77 K were obtained by using the spectral mode of the LP920 laser flash photolysis spectrometer, and the samples were excited at 355 nm. Figure 3 shows the spectra of **1**, which exhibit a clear vibronic

TABLE 1: Emission Data of 1 and 2 in Benzene

complex	λ_{em}/nm (τ_s/ns)[a] (298 K)	λ_{em}/nm (τ_s/μs)[b] (77 K)
1	789 (2.50, 75%; 6.47, 25%), 829	785 (34.0), 830 (28.0), 890 (30.0)
2	787 (2.16, 73%; 5.76, 27%), 828	782 (30.0), 830 (27.0), 884 (28.0)

[a] The excitation wavelength is 695 nm for **1** and 696 nm for **2** in benzene. [b] The excitation wavelength is 355 nm.

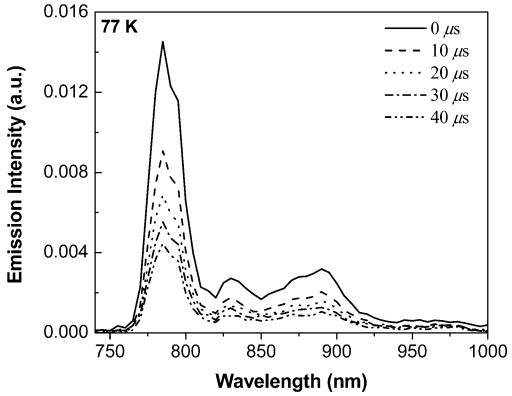

Figure 3. Time-resolved emission spectra of **1** at 77 K in glassy benzene. The excitation wavelength is 355 nm.

progression and a mirror image shape of that of the Q-band in its UV−vis spectrum. The emission peaks are almost identical to those measured at room temperature. Therefore, the low-temperature emission is also attributed to fluorescence. However, due to the reduced nonirradiative decay at 77 K, the emission lifetime is significantly increased. It is about 30.7 μs for **1**. The octabrominated complex **2** exhibits similar features with a lifetime of 28.3 μs (see Table 1) at 77 K.

Triplet Excited-State Characteristics. The time-resolved triplet transient difference absorption spectra of **1** and **2** in degassed benzene were obtained with an Edinburg LP920 laser flash photolysis spectrometer. As shown in Figure 4, **1** exhibits a positive band between 390 and 690 nm, while the positive band of **2** is broader, extending from 375 to 730 nm. On the other hand, both complexes show similar negative bands from 680 to 820 nm, which are due to the bleaching of the Q-band. From the decay of the transient absorption, the lifetime of the lowest triplet excited-state is extrapolated. Complex **1** exhibits a monoexponential decay with a lifetime of 67 μs at λ_{T1-Tn} = 610 nm. In contrast, complex **2** exhibits a biexponential decay at 610 nm, with a longer lifetime of 49 μs (94%) and a shorter one of 2.3 μs (6%). The shorter lifetime of **2** could possibly arise from the aggregated species that is more feasible to form in **2** due to the lack of bulky phenoxyl peripheral substituents and the higher polarity of the C−Br bonds.[2g,14] The presence of eight heavy peripheral bromides also leads to a rapid intersystem crossing from the first singlet excited state to the first triplet excited state and thus a rapid transition from the triplet excited state back to the ground state as well. Subsequently, the lifetime of the triplet excited state decreases as the number of peripheral bromide substituents increases, which is known as the heavy-atom effect.[13f,20] Similar results have been observed for octabrominated porphyrins as well.[13e]

The extinction coefficient for the triplet−triplet absorption (ϵ_T) was measured and calculated using the singlet depletion method.[16] The measurement of the depopulation was made in correspondence with the Q-band, where the extinction coefficients of the excited states (both singlet and triplet) are reasonably assumed to be negligible compared to that of the ground state. This method has been used successfully for group IA phthalocyanines, group IA naphthalocyanines,[21] and group IIIA phthalocyanines.[22] The extinction coefficients and the triplet excited-state quantum yields (Φ_T) are listed in Table 2. It is clear that the triplet quantum yield for **2** is larger than that of **1**. This is likely the result of the heavy-atom effect. The large number of heavy bromine atoms in the peripheral ring induces the fast intersystem crossing and thus increases the quantum yield of formation of the triplet excited state.

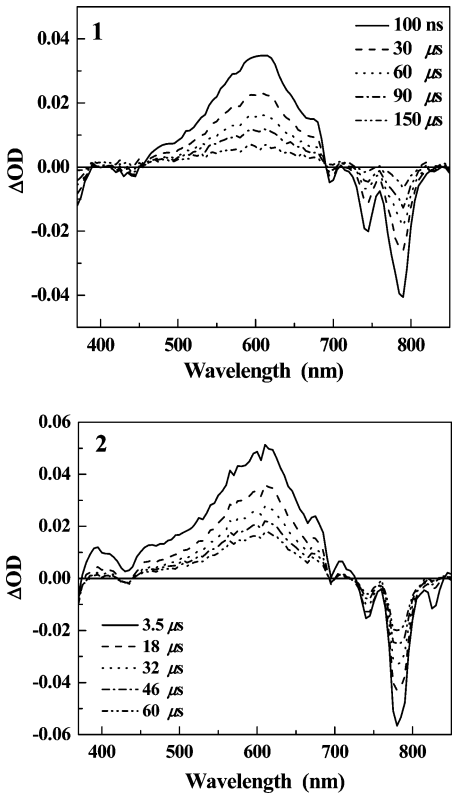

Figure 4. Time-resolved triplet transient difference absorption spectra of **1** and **2** in benzene. The time listed in the figures is the time delay after the 355 nm excitation.

TABLE 2: Triplet Excited-State Parameters of Complexes 1 and 2 in Benzene

complex	λ_{T1-Tn}/nm	τ_T/μs	ϵ_T/M^{-1} cm^{-1}	Φ_T	Φ_Δ
1	610	67	99960	0.10	0.16
2	610	49 (89%), 2.3 (11%)	94220	0.13	0.16

Singlet Oxygen Generation. Many metallophthalocyanines and metallonaphthalocyanines have been reported to generate singlet oxygen ($^1\Delta_g$), which is generally recognized as a key intermediate in photodynamic therapy (PDT), through energy transfer from their triplet excited states to the ground-state oxygen ($^3\Sigma_g^-$). This process enables these complexes to be promising photosensitizers for PDT applications.[4h,23] The singlet oxygen quantum yield (Φ_Δ) measures the efficiency of a photosensitizer to generate singlet oxygen. It usually relates to the triplet quantum yield Φ_T, triplet lifetime τ_T, triplet energy E_T, and energy transfer efficiency from the triplet excited state of the sensitizer to the ground state of molecular oxygen.[4h]

As described in the Experimental Section, the singlet oxygen generation was monitored by measuring the emission of the singlet oxygen at 1270 nm. As shown in Figure 5, a weak signal was observed in an air-saturated benzene solution of complex **2** at 1270 nm. This signal disappears upon degassing with argon. A similar phenomenon was also found for complex **1** in a benzene solution. Therefore, the generation of singlet oxygen

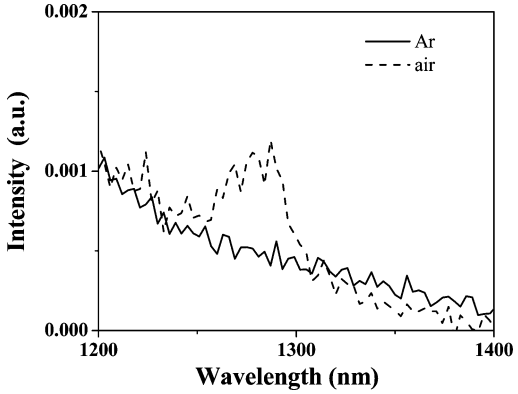

Figure 5. Emission spectrum of singlet oxygen generated by **2** in benzene at room temperature: Ar-saturated solution (solid line); air-saturated solution (dashed line).

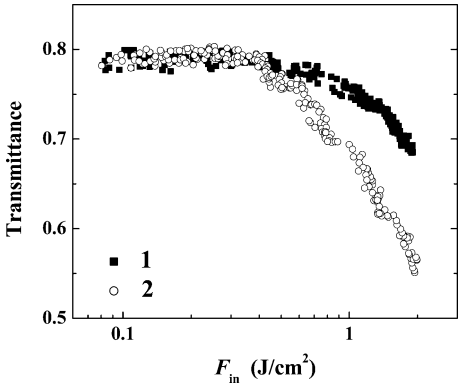

Figure 6. Nonlinear transmission curves of **1** and **2** for nanosecond pulses at 532 nm. The linear transmission at 532 nm for both solutions is adjusted to 80%. The cuvette used is 2 mm.

is clearly evident. The singlet oxygen quantum yield (Φ_Δ) was then measured by a comparative method as described in the Experimental Section, and the results are listed in Table 2. Complex **2** exhibits the same quantum yield of singlet oxygen generation as complex **1** although the triplet excited-state quantum yield of **2** is higher than that of **1**. This indicates that the variation of the number of peripheral bromides has a negligible effect on the Φ_Δ value and the energy transfer efficiency ($S_\Delta = \Phi_\Delta/\Phi_T$) from the triplet excited state to ground-state oxygen for **2** is lower than that of **1**.

It is worthy of mention that the calculated S_Δ values for these two complexes are larger than 1, which is unexpected. This is possibly due to the error in the triplet extinction coefficient measurement, which was subsequently used for calculating Φ_T. The singlet depletion method usually gives a high limit for the value of ϵ_T.[16,24] The higher value beyond expectation is probably due to the ground-state extinction coefficients that are not negligible at the transient absorption spectrum band maximum ($\lambda = 610$ nm). Nevertheless, the near-unity value of S_Δ for these two complexes suggests that the energy transfer efficiency from the triplet excited state to the ground-state oxygen is quite high.

Nonlinear Transmission. The triplet−triplet transient difference absorption spectra (Figure 4) of **1** and **2** exhibit a positive absorption at 532 nm, indicating that the excited-state absorption of both complexes is stronger than that of the ground state. In addition, both complexes possess a long-lived triplet excited state. In this case, reverse saturable absorption,[2,13,15] i.e., the increase of absorbance with the increase of incident energy, is expected for nanosecond laser pulses.

As shown in Figure 6, the transmittance of **1** and **2** decreases with the increase of the incident fluence at 532 nm. The threshold of the nonlinear transmission, defined as the incident fluence at which the transmittance starts to deviate from the linear transmittance, is 0.4 J/cm^2 for **2** and 0.8 J/cm^2 for **1**. The transmittance drops to 56% when the incident fluence increases to 1.8 J/cm^2 for **2** and 70% for **1** at a similar incident fluence. Octabrominated naphthalocyanine **2** shows stronger nonlinear transmission than tetrabrominated complex **1** at 532 nm, which coincides with the larger triplet excited-state quantum yield. Although complex **1** has a longer triplet lifetime than complex **2**, this lifetime is not the determining factor for the nonlinear transmission of nanosecond laser pulses as long as the excited-state lifetime is longer than the laser pulse width. The stronger nonlinear transmission observed for **2** is probably due to the larger ratio of excited-state absorption to ground-state absorption cross-sections at 532 nm, although the slightly larger triplet excited-state quantum yield of **2** could also contribute to its stronger nonlinear transmission. Due to the larger ground-state absorption of **1** and **2** at 532 nm, the nonlinear transmission behavior of these two complexes becomes much weaker at this wavelength compared to that of the corresponding unsubstituted SiNc.

Z-Scan. It is well-known that both nonlinear absorption and nonlinear refraction contribute to the third-order nonlinearities. The nonlinear transmission experiment discussed in the previous section only measures the contribution from the nonlinear absorption. It has been reported that some phthalocyanines and naphthalocyanines exhibit both nonlinear absorption and nonlinear refraction when irradiated with nanosecond and shorter laser pulses.[13a] To measure the contribution from nonlinear refraction of **1** and **2** and to quantitatively determine the excited-state absorption cross-sections, Z-scan[25] experiments are conducted.

In a Z-scan experiment, the nonlinear absorption and nonlinear refraction can be measured simultaneously. Nonlinear refraction is measured through a closed-aperture Z-scan, and nonlinear absorption is obtained through an open-aperture Z-scan. The closed-aperture Z-scan measures the on-axis phase change ($\Delta\Phi_0$) of a laser beam when it propagates through a nonlinear medium, which is related to the nonlinear refractive index (n_2) and the nonlinear refractive cross-section (σ_r) of a third-order nonlinear optical material by the following equation:[25,26]

$$n_2(m^2/W) = (\Delta\Phi_0)\lambda/2\pi L_{eff} I_0 \quad (4)$$

$$\Delta\Phi_0 = \frac{\alpha}{2h\nu}\sigma_r F_0 L_{eff} \quad (5)$$

where $L_{eff} = (1 - e^{\alpha L})/\alpha$ is the effective beam path with α as the linear absorption coefficient and I_0 is the on-axis ($r = 0$), peak ($t = 0$) irradiance with the nonlinear medium at the focal plane ($Z = 0$). For a Gaussian spatial and temporal distribution, $I_0 = 4(\ln 2)^{1/2}E_{total}/(\pi^3)^{1/2}\omega_0^2\tau$ and $F_0 = 2E_{total}/\pi\omega_0^2$, where E_{total} is the incident energy on the sample after the reflection from the front surface of the cell is taken into account, ω_0 is the radius of the beam waist at the focal point, and τ is the pulse width (full width at half-maximum). For a Gaussian beam Z-scan, $\Delta\Phi_0$ can be obtained from the fitting of the normalized nonlinear refraction curve (closed-aperture/open-aperture) using the following equation:[25]

$$T(z,\Delta\Phi) = 1 - \frac{4(\Delta\Phi)(z/z_0)}{[(z/z_0)^2 + 1][(z/z_0)^2 + 9]} \quad (6)$$

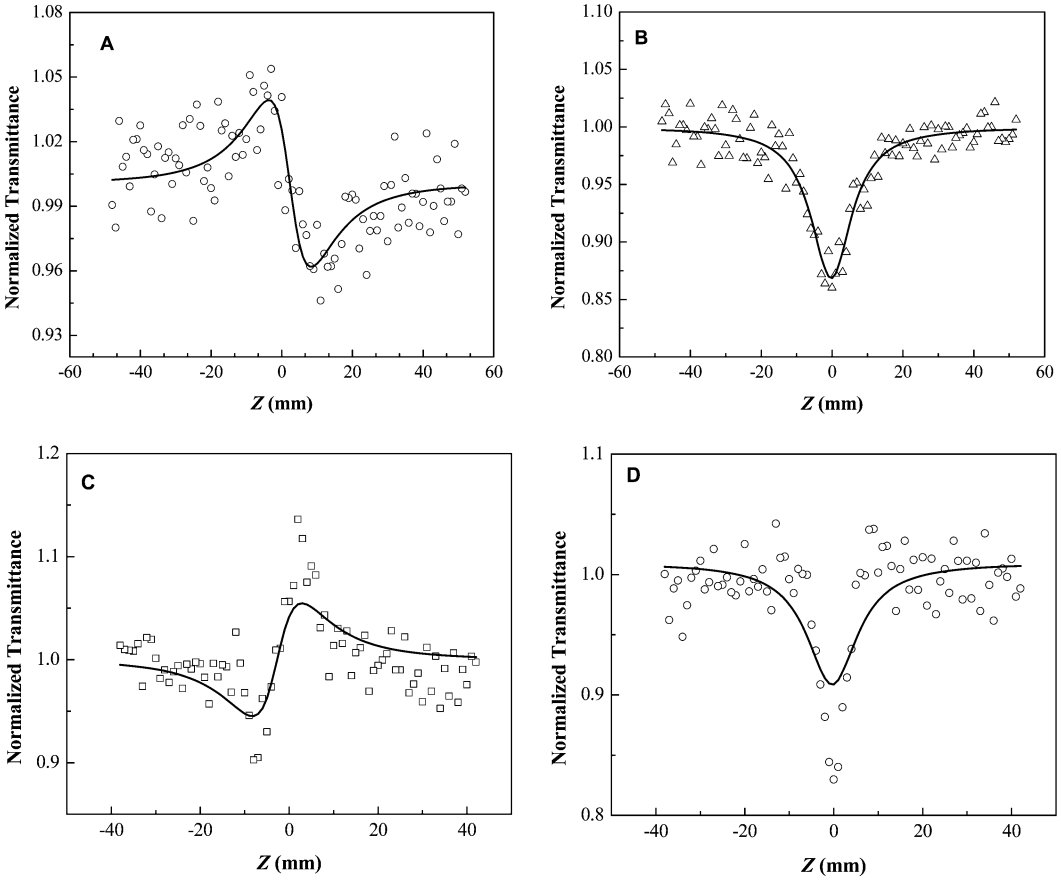

Figure 7. Nanosecond Z-scan curves of complexes **1** and **2** at 532 nm: (A) closed-aperture/open-aperture curve of **1**; (B) open-aperture curve of **2**; (C) closed-aperture/open-aperture curve of **2**; (D) open-aperture curve of **2**. The pulse energy used in the experiment is 6.0 μJ, and the path length of the cuvette is 1 mm.

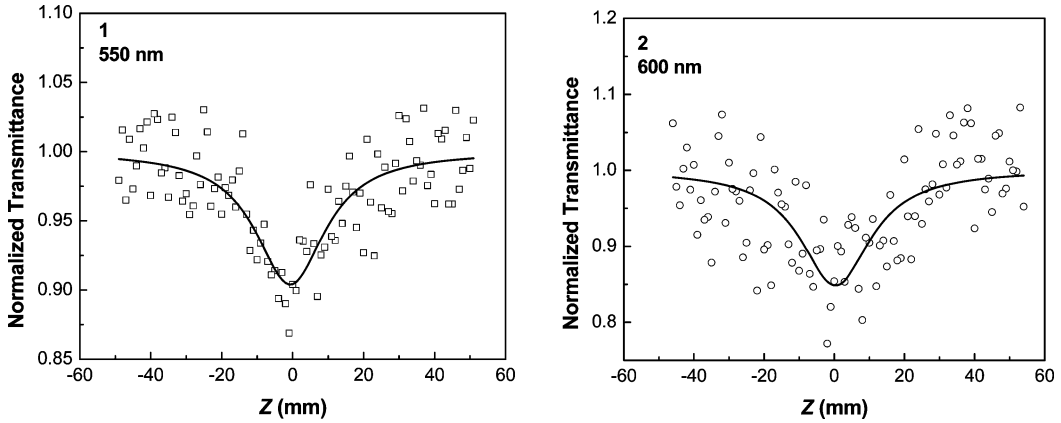

Figure 8. Open-aperture Z-scan curves for complexes **1** and **2** using picosecond laser pulses. The pulse energy is 1.8 μJ, and the cuvette used is 2 mm.

where T is the normalized transmission, z is the distance of the sample relative to the focal plane, and z_0 is the Rayleigh length.

As shown in Figure 7 for a nanosecond Z-scan, the pure nonlinear refraction curve displays a peak−valley shape for **1** and a valley−peak shape for **2**, indicating that **1** is a self-defocusing material and **2** is a self-focusing material for nanosecond laser pulses at 532 nm. By fitting this curve with eq 6, the on-axis phase change can be obtained. The nonlinear refractive index, n_2, is then calculated to be -2.3×10^{-17} m^2/W for **1** and 3.3×10^{-17} m^2/W for **2**, and the molecular nonlinear refractive cross-section is obtained to be -1.6×10^{-18} cm^2 for **1** and 2.2×10^{-18} cm^2 for **2**. Therefore, variation of the number of peripheral bromide substituents changes not only the sign of the nonlinear refractive index, but also the magnitude of the nonlinear refraction.

From the open-aperture Z-scan data, a significant transmission drop was observed for both complexes when the sample was moved toward the focal plane. This indicates a reverse saturable absorption. For a Gaussian beam Z-scan, the excited-state absorption cross-section can then be deduced from the fitting of the open-aperture curve using eq 7,[27] where $q_0 = \sigma_{es}\alpha[F_0(r = 0)]L_{eff}/2\hbar\omega$, with $L_{eff} = (1 - e^{-\alpha L})/\alpha$ and $F_0 = 2E_{total}/\pi\omega_0^2$. This gives rise to $\sigma_{ex} = 2.7 \times 10^{-18}$ cm^2 for **1** and $\sigma_{ex} = 1.9 \times$

$$T = \ln\left(1 + \frac{q_0}{1 + x^2}\right)\Big/\left(\frac{q_0}{1 + x^2}\right) \qquad (7)$$

TABLE 3: Singlet Excited-State Absorption Cross-Sections of 1 and 2 at Different Wavelengths Measured by Picosecond Z-Scans

	λ (nm)	σ_s (10^{-18} cm^2)
1	532	8.0
	550	12.0
2	532	4.3
	570	11.0
	600	21.0
	650	29.0

10^{-18} cm^2 for **2**, where σ_0 is determined by $\alpha = 10^{-3}\sigma_0 N_A C$. For nanosecond laser pulses, the nonlinear absorption is usually dominated by the triplet excited-state absorption. Therefore, the resulting σ_{ex} should mainly be attributed to σ_T. It is noteworthy that the theoretical curve does not fit well to the experimental data of **2**, especially for the data points obtained at the vicinity of the focal plane. This could arise from the contribution of higher excited states,[13a] or alternatively, it could be due to a dynamic of excited-state formation that is not taken into account in eq 7. To obtain a better fitting, a model that considers the decay and population of multiple excited states should be built up.

The picosecond Z-scan has also been carried out for these two complexes at several different wavelengths. As shown in Figure 8 for **1** and **2** at 550 and 600 nm, respectively, both complexes exhibit reverse saturable absorption for picosecond laser pulses. However, nonlinear refraction was not observed for either of these two samples. Fitting of the open-aperture curves with eq 7 produces a value of σ_{ex} that mostly depends on the absorption cross-section of the singlet excited state (σ_s). The σ_s values for **1** and **2** at different wavelengths are listed in Table 3. It is evident that the singlet excited-state absorption cross-section increases with the wavelength in the wavelength range examined.

Conclusions

The photophysical parameters and nonlinear optical properties of two newly synthesized silicon naphthalocyanines, namely, tetrabrominated $Br_4(tBu_2PhO)_4NcSi[OSi(Hex)_3]_2$ (**1**) and octabrominated $Br_8NcSi[OSi(Hex)_3]_2$ (**2**), have been investigated. In particular, the molar extinction coefficients of the ground and excited states, the quantum yield of the excited-state formation, the lifetime of the triplet excited state, the singlet oxygen generation quantum yield, and the transient absorption spectra of **1** and **2** were measured and calculated. The increased number of peripheral bromides from **1** to **2** results in the shortening of the triplet excited-state lifetime and the increase of the quantum yield of the triplet excited-state formation, as expected on the basis of the heavy-atom effect. The enhanced nonlinear transmission behavior of the octabrominated complex **2** could be ascribed to the increased ratio of the triplet excited-state absorption to ground-state absorption cross-sections, although the slightly increased triplet excited-state quantum yield of **2** could also play a role. In addition, the variation of the peripheral bromide substituents influences both the sign and the magnitude of the nonlinear refraction of these two complexes for nanosecond laser pulses at 532 nm.

Acknowledgment. Financial support from the NSF NIRT program (Grant DMI-0506531) for W.S. and Y.L. and from EU (Contracts HPRN-CT-2000-00020 and HPRN-CT-2002-00323) for D.D. and M.H. is gratefully acknowledged.

References and Notes

(1) (a) Gouterman, M. *J. Mol. Spectrosc.* **1961**, *6*, 138−163. (b) Orti, E.; Crespo, R.; Piqueras, M. C.; Viruela, P. M.; Tomas, F. *Synth. Met.* **1993**, *57*, 4513−4518. (c) Kobayashi, N.; Nakajima, S. I.; Osa, T. *Inorg. Chim. Acta* **1993**, *210*, 131−133. (d) Yousaf, M.; Lazzouni, M. *Dyes Pigments* **1995**, *28*, 69−75. (e) Guyon, F.; Pondaven, A.; Kerbaol, J.-M.; L'Her, M. *Inorg. Chem.* **1998**, *37*, 569−576. (f) Andzelm, J.; Rawlett, A. M.; Orlicki, J. A.; Snyder, J. F.; Baldridge, K. K. *J. Chem. Theory Comput.* **2007**, *3*, 870−877.

(2) (a) Wang, N. Q.; Cai, Y. M.; Heflin, J. R.; Wu, J. W.; Rodenberger, D. C.; Garito, A. F. *Polymer* **1991**, *32*, 1752−1755. (b) Williams, G. R. J. *J. Mol. Struct.: THEOCHEM* **1995**, *332*, 137−140. (c) Swatton, S. N. R.; Welford, K. R.; Hollins, R. C.; Sambles. J. R. *Appl. Phys. Lett.* **1997**, *71*, 10−12. (d) Shirk, J. S.; Pong, R. G. S.; Flom, S. R.; Bartoli, F. J.; Boyle, M. E.; Snow, A. R. *Pure Appl. Opt.* **1996**, *5*, 701−707. (e) Nalwa, H. S.; Hanack, M.; Pawlowski, G.; Engel, M. K. *Chem. Phys.* **1999**, *245*, 17−26. (f) Pittman, M.; Plaza, P.; Martin, M. M.; Meyer, Y. H. *Opt. Commun.* **1998**, *158*, 201−212. (g) Hanack, M.; Schneider, T.; Barthel, M.; Shirk, J. S.; Flom, S. R.; Pong, R. G. S. *Coord. Chem. Rev.* **2001**, *219*, 235−258. (h) Robertson, J.; Smith, A.; Duignan, J.; Milsom, P.; Bourhill, G. *Appl. Phys. Lett.* **2001**, *78*, 1183−1185. (i) Unnikrishnan, K. P.; Thomas, J.; Nampoori, V. P. N.; Vallabhan, C. P. G. *Chem. Phys.* **2002**, *279*, 209−213. (j) Unnikrishnan, K. P.; Thomas, J.; Nampoori, V. P. N.; Vallabhan, C. P. G. *Opt. Commun.* **2002**, *204*, 385−390. (k) Chen, Y.; O'Flaherty, S.; Fujitsuka, M.; Hanack, M.; Subramanian, L. R.; Ito, O.; Blau, W. J. *Chem. Mater.* **2002**, *14*, 5163−5168. (l) Yang, G. Y.; Hanack, M.; Lee, Y. W.; Chen, Y.; Lee, M. K. Y.; Dini, D. *Chem.—Eur. J.* **2003**, *9*, 2758−2762. (m) Fu, G.; Yoda, T.; Kasatani, K.; Okamoto, H.; Takenaka, S. *Synth. Met.* **2005**, *155*, 68−72. (n) Chen, Y.; Hanack, M.; Araki, Y.; Ito, O. *Chem. Soc. Rev.* **2005**, *34*, 517−529. (o) Nalwa, H. S.; Kakuta, A.; Mukoh, A. *J. Phys. Chem.* **1993**, *97*, 1097−1100. (p) Sun, W.; Wang, G.; Li, Y.; Calvete, M. J. F.; Dini, D.; Hanack, M. *J. Phys. Chem. A* **2007**, *111*, 3263−3270. (q) De la Torre, G.; Vazquez, P.; Agullo-Lopez, F.; Torres, T. *Chem. Rev.* **2004**, *104*, 3723−3750. (r) O'Flaherty, S. M.; Hold, S. V.; Cook, M. J.; Torres, T.; Chen, Y.; Hanack, M.; Blau, W. J. *Adv. Mater.* **2003**, *15*, 19−32.

(3) (a) Hanack, M.; Deger, S.; Keppeler, U.; Lange, A.; Leverenz, A.; Rein, M. *Synth. Met.* **1987**, *19*, 739−744. (b) Hanack, M.; Linge, A.; Rein, M.; Behnisch, R.; Renz, G.; Leverenz, A. *Synth. Met.* **1989**, *29*, 1−8. (c) Bouvet, M.; Simon, J. *Chem. Phys. Lett.* **1990**, *172*, 299−302. (d) Hanack, M.; Lange, A.; Grosshans, R. *Synth. Met.* **1991**, *45*, 59−70. (e) Hayashida, S.; Hanack, M. *Synth. Met.* **1991**, *52*, 241−255.

(4) (a) Darwent, J. R.; Douglas, P.; Harriman, A.; Porter, G.; Richoux, M. C. *Photochem. Photobiol.* **1987**, *45*, 535−538. (b) Zuk, M. M.; Rihter, B. D.; Kenney, M. E.; Rodgers, M. A. J.; Kreimer-Birnbaum, M. *J. Chromatogr., B* **1991**, *568*, 437−444. (c) Jori, G. *J. Photochem. Photobiol., A* **1992**, *62*, 371−378. (d) Krasnovsky, A. A.; Rodgers, M. A.; Galpern, M. G.; Rihter, B.; Kenney, M. E.; Lukjanetz, E. A. *Photochem. Photobiol.* **1992**, *55*, 691−696. (e) Zuk, M. M.; Rihter, B. D.; Kenney, M. E.; Rodgers, M. A.; Kreimer-Birnbaum, M. *Photochem. Photobiol.* **1994**, *59*, 66−72. (f) Brasseur, N.; Nguyen, T. L.; Langlois, R.; Ouellet, R.; Marengo, S.; Houde, D.; Van Lier, J. E. *J. Med. Chem.* **1994**, *37*, 415−420. (g) Ford, W. E.; Rihter, B. D.; Kenney, M. E.; Rodgers, M. A. J. *J. Am. Chem. Soc.* **1989**, *111*, 2362−2363. (h) Firey, P. A.; Ford, W. E.; Sounik, J. R.; Kenney, M. E.; Rodgers, M. A. J. *J. Am. Chem. Soc.* **1988**; *110*, 7626−7630. (i) Marengo, S.; Houde, D.; Brasseur, N.; Nguyen, T. L.; Ouellet, R.; Van Lier, J. E. *J. Chim. Phys. Phys.-Chim. Biol.* **1994**, *91*, 1211−1218.

(5) (a) Darwent, J. R.; Douglas, P.; Harriman, A.; Porter, G.; Richoux, M. C. *Coord. Chem. Rev.* **1982**, *44*, 83−126. (b) Dieng, M.; Contamin, O.; Savy, M. *Electrochim. Acta* **1988**, *33*, 121−126. (c) Biloul, A.; Coowar, F.; Contamin, O.; Scarbeck, G.; Savy, M.; Van den Ham, D.; Riga, J.; Verbist, J. J. *J. Electroanal. Chem.* **1990**, *289*, 189−201.

(6) (a) Hayashida, S.; Hayashi, N. *Synth. Met.* **1991**, *41*, 1243−1248. (b) Hayashida, S.; Hayashi, N. *Chem. Mater.* **1991**, *3*, 92−95.

(7) Volcker, A.; Adick, H. J.; Schmidt, R.; Brauer, H. D. *Chem. Phys. Lett.* **1989**, *159*, 103−108.

(8) Yousaf, M.; Lazzouni, M. *Dyes Pigments* **1995**, *27*, 297−303.

(9) Hisao, Y.; Takashi, K.; Michio, A. *J. Appl. Phys.* **1993**, *73*, 3812−3819.

(10) Turukhin, A. V.; Gorokhovsky, A. A.; Moser, C.; Solomatin, I. V.; Psaltis, D. *J. Lumin.* **2000**, *86*, 399−405.

(11) Waddell, E.; Wang, Y.; Stryjewski, W.; McWhorter, S.; Henry, A. C.; Evans, D.; McCarley, R. L.; Soper, S. A. *Anal. Chem.* **2000**, *72*, 5907−5917.

(12) (a) Wheeler, B. L.; Nagasubramanian, G.; Bard, A. J.; Schechtman, L. A.; Kenney, M. E. *J. Am. Chem. Soc.* **1984**, *106*, 7404−7410. (b) Ford, W. E.; Rodgers, M. A. J.; Schechtman, L. A.; Sounik, J. R.; Rihter, B. D.; Kenney, M. E. *Inorg. Chem.* **1992**, *31*, 3371−3377. (c) Polley, R.; Hanack, M. *J. Org. Chem.* **1995**, *60*, 8278−8282. (d) Gacho, E. H.; Imai, H.; Tsunashima, R.; Naito, T.; Inabe, T.; Kobayashi, N. *Inorg. Chem.* **2006**, *45*, 4170−4176.

(13) (a) Dini, D.; Calvete, M. J. F.; Hanack, M.; Pong, R. G. S.; Flom, S. R.; Shirk, J. S. *J. Phys. Chem. B* **2006**, *110*, 12230−12239. (b) Dini, D.; Calvete, M.; Vagin, S.; Hanack, M.; Eriksson, A.; Lopes, C. *J. Porphyrins Phthalocyanines* **2006**, *10*, 1165−1171. (c) Ye, H.; Chang, Q.; Wu, Y.; He, C.; Zuo, X.; Zhan, J.; Wang, Y.; Song, Y. *Mater. Lett.* **2003**, *57*, 3302−

3304. (d) Song, Y.; Wang, Y.; Li, J.; Fang, G.; Yang, X.; Wu, Y.; Liu, Y.; Zuo, X.; Zhu, Q.; Chen, N. *Proc. SPIE-Int. Soc. Opt. Eng.* **1998**, *3554*, 241−245. (e) Su, W.; Cooper, T. M.; Brant, M. C. *Chem. Mater.* **1998**, *10*, 1212−1213. (f) Bonnett, R.; Harriman, A.; Kozyrev, A. N. *J. Chem. Soc., Faraday Trans.* **1992**, *88*, 763−769. (g) Mandon, D.; Ochsenbein, P.; Fischer, J.; Weiss, R.; Jayaraj, K.; Austin, R. N.; Gold, A.; White, P. S.; Brigaud, O.; Battioni, P.; Mansuy, D. *Inorg. Chem.* **1992**, *31*, 2044−2049.

(14) (a) Snow, A. W.; Jarvis, N. L. *J. Am. Chem. Soc.* **1984**, *106*, 4706−4711. (b) Snow, A.W. In *The Porphyrin Handbook*; Kadish, K. M., Smith, K. M., Guilard, R., Eds.; Elsevier Science: Amsterdam, 2003; Vol. 17, pp 129−176. (c) Choi, M. T. M.; Li, P. P. S.; Ng, D. K. P. *Tetrahedron* **2000**, *56*, 3881−3887. (d) Li, Z.; Huang, X.; Xu, S.; Chen, Z.; Zhang, Z.; Zhang, F.; Kasatani, K. *J. Photochem. Photobiol., A* **2007**, *188*, 311−316.

(15) (a) Shirk, J. S.; Pong, R. G. S.; Flom, S. R.; Heckmann, H.; Hanack, M. *J. Phys. Chem. A* **2000**, *104*, 1438−1449. (b) Dini, D.; Barthel, M.; Schneider, T.; Ottmar, M.; Verma, S.; Hanack, M. *Solid State Ionics* **2003**, *165*, 289−303. Barthel, M.; Dini, D.; Vagin, S.; Hanack, M. *Eur. J. Org. Chem.* **2002**, 3756−3762. (c) Maya, E. M.; Snow, A. R.; Shirk, J. S.; Pong, R. G. S.; Flom, S. R.; Roberts, G. L. *J. Mater. Chem.* **2003**, *13*, 1603−1613. (d) Riggs, J. E.; Martin, R. B.; Walker, D. B.; Guo, Z.; Sun, Y. P. *Phys. Chem. Chem. Phys.* **2004**, *6*, 703−709. (e) Brusatin, G.; Innocenzi, P.; Guglielmi, M.; Signorini, R.; Bozio, R. *Mol. Cryst. Liq. Cryst. Sci. Technol., B* **2001**, *27*, 259−267.

(16) Carmichael, I.; Hug, G. L. *J. Phys. Chem. Ref. Data* **1986**, *15*, 1−250.

(17) (a) Bensasson, R.; Goldschmidt, C. R.; Land, E. J.; Truscott, T. G. *Photochem. Photobiol.* **1978**, *28*, 277−281. (b) Foley, S.; Jones, G.; Liuzzi, R.; McGarvey, D. J.; Perry, M. H.; Truscott, T. G. *J. Chem. Soc., Perkin Trans. 2* **1997**, *2*, 1725−1730.

(18) Sun, W.; Dai, Q.; Worden, J. G.; Huo, Q. *J. Phys. Chem. B* **2005**, *109*, 20854−20857.

(19) Shao, P.; Li, Y.; Sun, W. Submitted for publication to *J. Am. Chem. Soc*.

(20) Turro, N. J. *Modern Molecular Photochemistry*; University Science Books: Sausalito, CA, 1991; p 124.

(21) Gilat, S. L.; Ebbesen, T. W. *J. Phys. Chem*. **1993**, *97*, 3551−3554.

(22) Brannon, J. H.; Magde, D. *J. Am. Chem. Soc*. **1980**, *102*, 62−65.

(23) (a) Spikes, J. D. *J. Photochem. Photobiol., B* **1990**, *6*, 259−274. (b) Bonnett, R. *Chemical Aspects of Photodynamic Therapy*; Gordon and Breach Science: Canada, 2000. (c) Ogunsipe, A.; Nyokong, T. *J. Photochem. Photobiol., A* **2005**, *173*, 211−220. (d) McCubbin, I.; Phillips, D. *J. Photochem.* **1986**, *34*, 187−195. (e) Ogunsipe, A.; Chen, J.; Nyokong, T. *New J. Chem*. **2004**, *28*, 822−827.

(24) Bishop, S. M.; Beeby, A.; Meunier, H.; Parker, A. W.; Foley, M. S. C.; Phillips, D. *J. Chem. Soc., Faraday Trans.* **1996**, *92*, 2689−2695.

(25) Sheik-Bahae, M.; Said, A. A.; Wei, T. H.; Hagan, D. J.; Stryland, E. W. V. *IEEE J. Quantum Electron.* **1990**, *26*, 760−769.

(26) Stryland, E. W. V.; Sheikbahae, M.; Said, A. A.; Hagan, D. *Proc. SPIE-Int. Soc. Opt. Eng.* **1993**, *1852*, 135−150.

(27) Wood, J. L.; Miller, M. J.; Mott, A. G. *Opt. Lett*. **1995**, *20*, 973−975.